SEISMIC ATTENUATION AT DEPTH: LSST ARRAY, HUALIEN, TAIWAN

Bruno HERNANDEZ[(1)], Julie ALBARIC[(2)] and Yoshimitsu FUKUSHIMA[(3)]

[(1)] CEA, DAM, DIF, F-91297 Arpajon, France

[(2)] Bourgogne Franche-Comté University, Besançon, France

[(3)] International Atomic Energy Agency, Vienna, Austria

E-mail contact of main author: bruno.hernandez@cea.fr

Abstract. Seismic downhole-array data provide a unique source of information on actual seismic attenuation at shallow depth. Accelerograms of 51 events recorded at 10 seismic stations from two of the three vertical borehole of the Large Scale Seismic Test (LSST) array Hualien (Taiwan), are used to perform a regression analysis. The aim is to derive an attenuation relationship with depth ranging from the surface down to 53 m in depth. Analyses were conducted on both peak ground acceleration and acceleration response spectra (from 0.1 to 33 Hz). These attenuation relations show that, compared with surface ground motion, subsurface accelerations are lower by a factor 1 to 4 according to the depth and the frequency band. Ratios between the receiver responses obtained at different depths provide average transfer functions. Those are compared with transfer functions calculated by averaging ratios of observed response spectra between each depth and the surface. A good agreement between the two techniques is found. Finally, theoretical transfer functions are estimated using one-dimensional SH modeling. They are in good agreement with the data.

Key Words: seismic attenuation, depth, site effect, LSST array, Hualien, Taiwan.

1. Introduction

The analysis of subsurface seismic data is useful in order to quantify the potential benefits in term of seismic hazard of the subsurface domain. It is important to study the characteristics of shallow seismic motion and particularly, their main differences in comparison with the surface motion in order to estimate the seismic hazard for subsurface installations.

In this paper we present a statistical analysis of the seismic motion variation with depth applied to two vertical arrays of the Hualien Large Scale Seismic Test (LSST). This study aims at demonstrating the effects of the free-surface, near-surface velocity gradients, and low impedance surface layers on the amplitudes of seismic waves.

2. The strong motion Database

2.1. The Hualien Large Scale Seismic Test

The Hualien LSST was initiated in 1993 by a consortium of industrial and research enterprises from five countries (Japan, USA, Taiwan, France and Korea). This experiment includes 3 seismic downhole arrays (Figure 1).

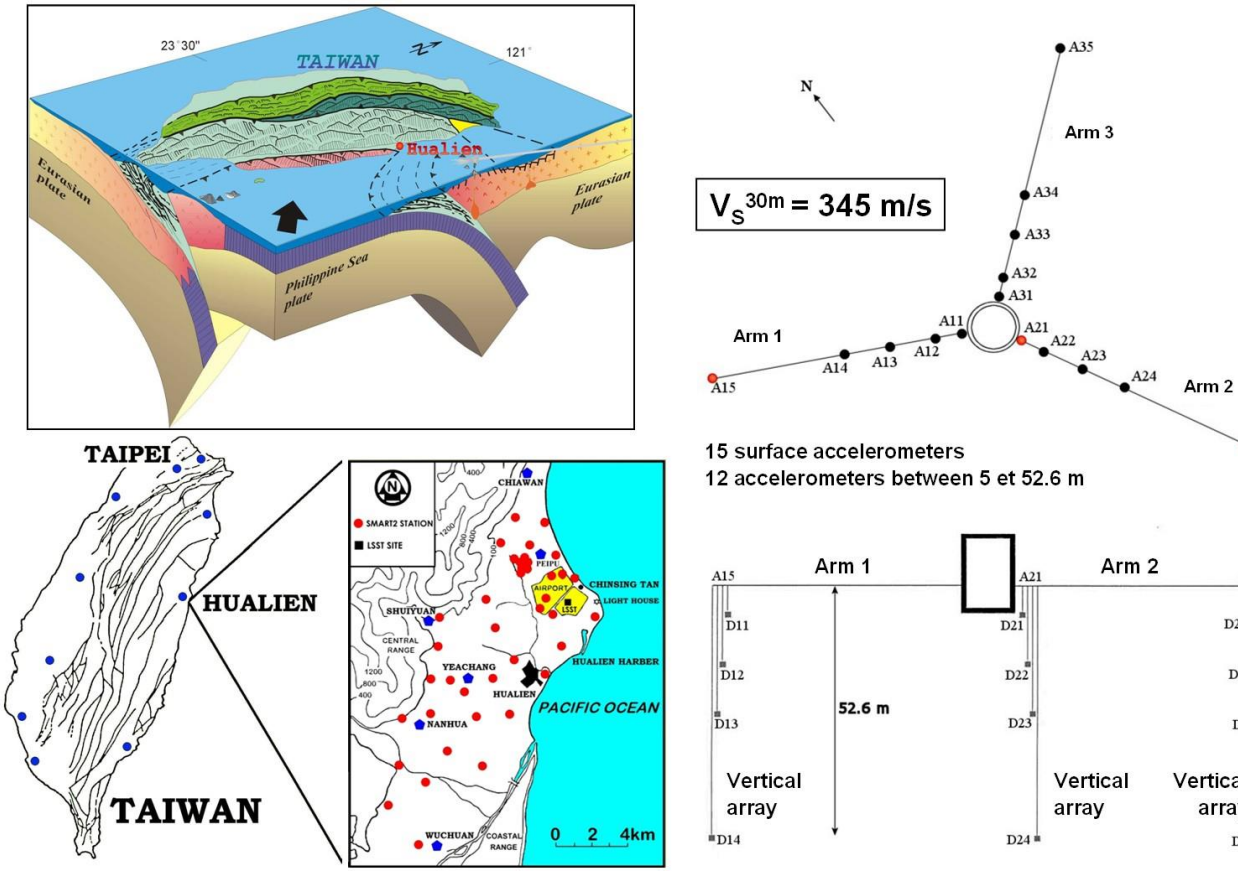

Figure 1. The Hualien LSST is located on the east coast of Taiwan in a highly active seismic zone (Geodynamic context from Angelier, 1986). The ground instrumentation included 15 surface accelerometers along Arm1, Arm2 and Arm3 and 3 subsurface downhole arrays that extended to a depth of 52.6 m below the ground surface.

2.2. Seismotectonic context and site geology

The island of Taiwan lies along the boundary of the Philippine Sea and Eurasian tectonic plates (Figure 1). The Philippine Sea plate is moving at a velocity of the order of 7 cm/yr northwest toward the Eurasian plate where it subducts beneath the Eurasian plate along the Ryukyu Trench and overrides the Eurasian plate in the south along the Manila Trench. The Philippine Sea plate collides with the island of Taiwan forming an oblique plate boundary along the Longitudinal Valley fault zone that forms the extreme eastern edge of the island. The island of Taiwan, between these two subduction zones, results from the arc-continent collision. The important seismic activity observed at Taiwan is related to the pattern of the subduction and collision zones. The LSST Hualien site is located on the eastern coast of Taiwan, in a highly active seismic zone. Within a circle of 60 km, the annual number of earthquake with $M_L > 5.5$ is 6.4.

The geology at the LSST Hualien site consists of massive unconsolidated poorly bedded Pleistocene conglomerate composed of pebbled varying in diameter from 5 to 20 cm (Tang et al., 1991). Subsurface ground (about 5 m depth) is mainly composed of fine and medium sand. A gravel layer is located at a depth of about 5 m below ground surface and extends down to a depth of 40 m.

2.3. Seismic instrumentation

A lot of instruments were deployed to record seismic structural and ground responses and to monitor soil pore water pressure buildup. The surface instrumentation included 15 surface triaxial accelerometers along Arm1, Arm2 and Arm3 (Figure 3). The subsurface seismological instrumentation is composed of three downhole triaxial accelerometers arrays that extended down to a depth of 52.6 m below the ground surface.(Figure 3). One downhole array was located at the end of Arm1 (A15, D11, D12, D13, D14), and the other two vertical arrays were located at the beginning and end of Arm2 (A21, D21, D22, D23, D24 and A25, D25, D26, D27, D28). Downhole triaxial Sensors were installed at depths of 5.3, 15.8, 26.3 and 52.6 m.

2.4. Record selection and data processing

In this study, we only used the data recorded by the vertical network located at the end of Arm 1 and Arm 2.

From September 1993 to April 2002, 118 earthquakes were recorded by the HLSST networks including the Chichi earthquake of September 20, 1999 (Figure 2).

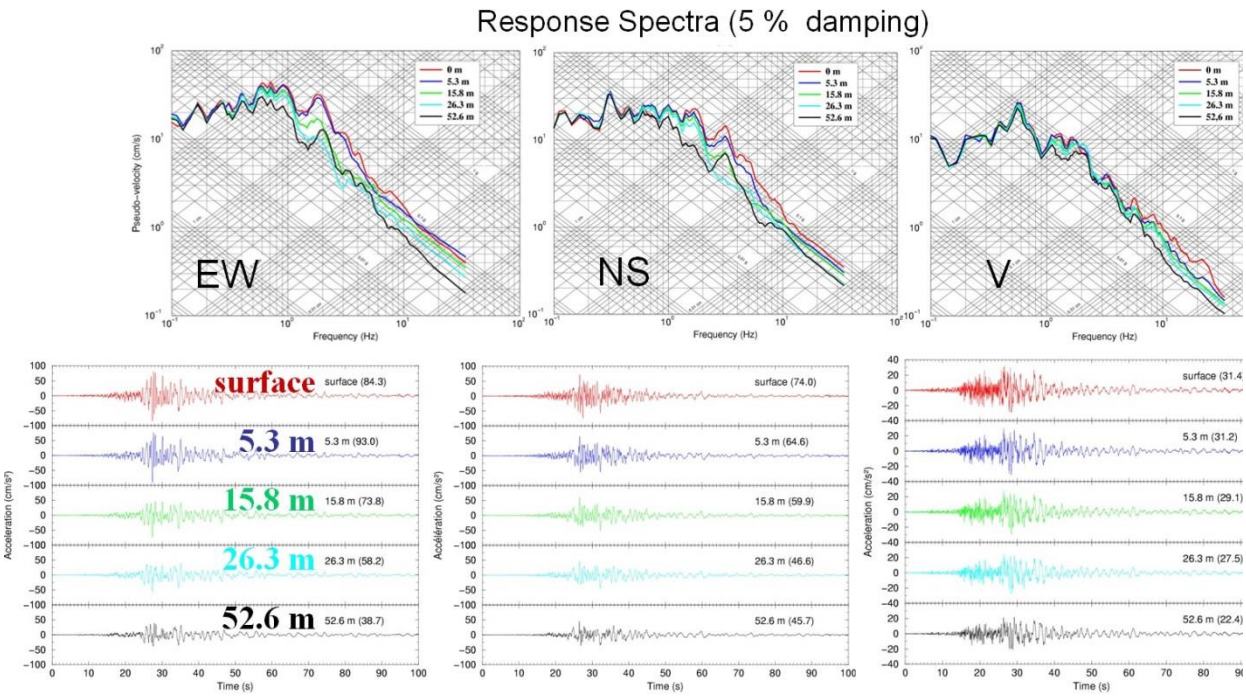

Figure 2. Response spectra and recorded acceleration time histories during the Chichi earthquake of September 21, 1999 (dark line in table I).

In order to achieve a uniform dataset, we performed a selection on records using the following criteria:

- M_L greater than 5.
- Focal depth lower than 30 km (superficial seismicity).
- $0.42\ M_L - \log(X + 0.025*10^{0.42ML}) - 0.0033X + 1.22 > \log 10$ (Fukushima et al., 2003)
  where M_L is the local magnitude and X is the hypocentral distance.

The Local magnitude of the selected events ranges from 5.0 to 7.3. These events are located between 5.5 km and 133.8 km in epicentral distance. A list of the events used in this

study is given on Table I and the epicenter locations are plotted on Figure 3. The magnitude-distance distribution of the selected dataset is shown on Figure 3.
All records were uniformly processed with a band-pass filter (0.08-40Hz).

Table I. Selected events description (M_L from CWB ; M_S and m_b from ISC)

ID	Date	h	'	''	Longitude	Latitude	$D_{Epi.}$	$D_{Hypo.}$	Z	M_L	M_S	m_b	Stations
4	19940605	1	9	30.100	121.8377	24.4623	54.3	54.6	5.3	6.2	6.6	6.0	9
6	19950223	5	19	2.780	121.6870	24.2037	21.9	30.9	21.7	5.8	6.2	5.9	10
12	19951218	16	17	54.530	121.6920	24.0183	7.5	23.3	22.1	5.8	5.0	5.1	8
13	19960305	14	52	27.130	122.3615	23.9302	76.1	76.3	6.0	6.4	6.5	6.0	10
14	19960305	17	32	8.560	122.3030	23.8985	70.8	71.6	10.8	6.0	5.8	5.6	10
15	19960528	21	53	22.350	121.5828	24.0535	5.5	25.6	25.0	5.1	4.7	4.7	10
16	19961126	8	22	23.710	121.6953	24.1643	18.2	31.9	26.2	5.3	4.8	4.9	9
25	19980717	4	51	14.960	120.6625	23.5027	112.8	112.9	2.8	6.2	5.6	5.4	5
33	19980904	10	40	50.600	121.5765	23.9140	12.2	16.4	11.0	5.0	4.1	4.6	3
38	**19990920**	**17**	**47**	**15.850**	**120.8155**	**23.8525**	**83.6**	**84.0**	**8.0**	**7.3**	**7.6**	**6.3**	**10**
39	19990920	17	57	15.580	121.0443	23.9117	59.5	60.0	7.7	6.4	5.7	6.0	9
40	19990920	17	58	55.130	121.0627	23.9070	57.8	58.2	7.0	5.7	-9.0	-9.0	9
41	19990920	18	3	41.570	120.8608	23.7968	80.8	81.4	9.8	6.6	6.6	6.1	9
42	19990920	18	11	54.210	121.0672	23.8648	58.5	59.8	12.5	6.7	6.2	6.1	9
43	19990920	18	16	17.950	121.0408	23.8615	61.2	62.5	12.5	6.7	6.3	6.0	9
44	19990920	20	40	3.820	121.3582	23.9622	27.1	27.6	5.2	5.1	5.0	4.9	9
45	19990920	20	43	48.750	121.3303	23.7615	40.8	41.7	8.8	5.2	4.9	4.7	9
46	19990920	21	46	38.110	120.8570	23.5847	91.2	91.6	8.6	6.6	6.5	5.8	9
49	19990921	7	6	2.660	121.3958	23.7980	33.2	35.1	11.4	5.4	4.4	5.0	9
52	19990921	17	38	35.570	121.3115	23.8373	37.0	41.0	17.7	5.2	4.4	5.1	9
53	19990921	22	16	59.770	121.3465	23.9313	29.2	29.2	1.1	5.3	4.6	5.0	9
54	19990922	0	14	40.770	121.0467	23.8263	61.9	63.8	15.6	6.8	6.4	6.0	9
55	19990922	0	49	43.450	121.0313	23.7647	65.9	68.2	17.4	6.2	5.9	5.7	9
56	19990922	2	19	29.610	121.3947	23.7887	34.1	36.1	12.0	5.4	4.4	4.8	9
59	19990923	12	44	33.690	121.0815	23.9122	55.8	56.2	6.5	5.7	4.8	5.2	9
60	19990923	21	39	0.100	121.3370	24.0005	28.7	28.7	1.4	5.4	4.3	4.8	9
61	19990925	8	43	31.100	120.9537	23.6920	76.6	77.0	7.1	5.1	4.9	5.0	9
62	19990925	23	52	49.630	121.0023	23.8542	65.2	66.3	12.1	6.8	6.5	6.1	9
63	19990927	11	55	7.060	121.3503	23.7075	43.9	45.2	10.7	5.2	4.9	5.2	9
64	19990927	18	10	0.490	121.3355	23.7963	37.8	39.4	11.3	5.0	4.2	4.5	9
67	19991001	12	54	10.280	120.9055	23.6940	80.9	81.1	5.2	5.1	4.8	4.8	9
69	19991005	12	18	17.370	121.0018	23.8448	65.5	66.3	9.9	5.0	-9.0	-9.0	9
71	19991013	1	39	46.880	121.3385	23.9552	29.3	29.3	1.9	5.0	5.4	5.3	9
73	19991018	15	31	26.870	121.3272	23.9492	30.5	30.8	4.3	5.0	4.5	4.9	9
74	19991018	16	0	45.890	121.0350	23.7048	68.7	72.7	23.8	5.2	4.8	4.9	9
75	19991022	2	18	56.900	120.4225	23.5170	133.8	134.8	16.6	6.4	5.7	5.6	9
76	19991022	3	10	17.460	120.4307	23.5330	132.3	133.3	16.7	6.0	5.3	5.1	9
79	19991030	8	27	49.500	121.3187	24.0172	30.5	30.8	4.4	5.2	4.6	5.0	9
84	20000506	13	41	52.840	121.5603	24.0235	6.0	27.6	27.0	5.1	-9.0	4.6	9
85	20000610	18	23	29.450	121.1092	23.9010	53.3	55.7	16.2	6.7	6.2	6.0	9
86	20000619	21	56	24.760	121.0922	23.9203	54.5	60.9	27.0	5.2	4.7	4.9	9
90	20000713	22	1	10.320	121.8268	23.9397	22.8	23.4	5.3	5.1	4.6	4.5	9
91	20000714	0	7	32.640	121.7283	24.0483	11.7	13.7	7.2	5.7	5.2	5.1	10
94	20000714	23	4	34.640	121.8032	23.9470	20.3	21.2	6.0	5.1	4.9	4.4	10

ID	Date	h	'	''	Longitude	Latitude	$D_{Epi.}$	$D_{Hypo.}$	Z	M_L	M_S	m_b	Stations
95	20000717	6	50	39.380	121.7898	24.0665	18.3	21.0	10.3	5.1	4.3	4.3	10
96	20000719	4	46	33.420	121.7602	24.1188	18.3	18.7	3.7	5.0	4.2	4.2	10
101	20000823	0	49	16.580	121.6347	23.6360	42.3	50.5	27.5	5.6	4.7	5.0	9
102	20000910	8	54	46.530	121.5838	24.0853	8.4	19.6	17.7	6.2	5.7	5.5	9
112	20001129	11	0	33.000	121.7682	23.8573	23.3	27.9	15.3	5.2	-9.0	-9.0	10
116	20020212	3	27	25.000	121.7227	23.7407	32.5	44.1	29.9	6.2	5.3	5.9	8
117	20020331	6	52	49.950	122.1915	24.1398	59.8	61.3	13.8	6.8	-9.0	-9.0	8

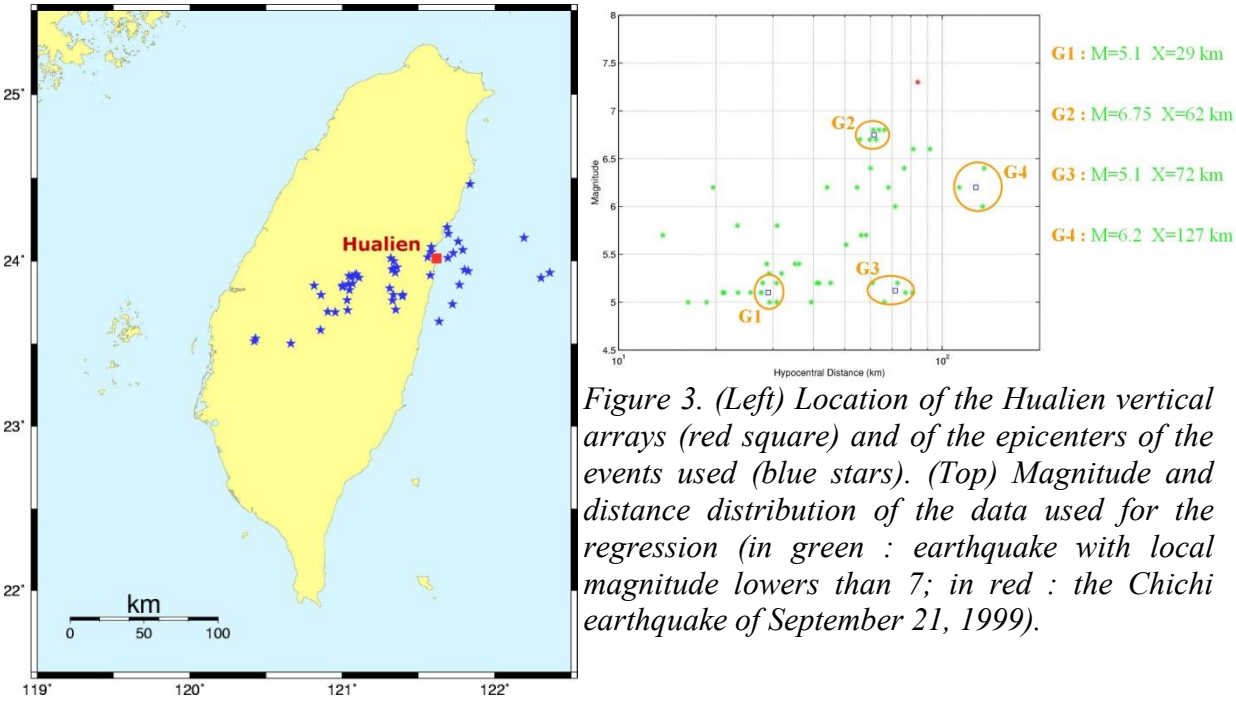

Figure 3. (Left) Location of the Hualien vertical arrays (red square) and of the epicenters of the events used (blue stars). (Top) Magnitude and distance distribution of the data used for the regression (in green : earthquake with local magnitude lowers than 7; in red : the Chichi earthquake of September 21, 1999).

3. Attenuation relation

The pseudo-acceleration response spectrum PSA(f) at 5% damping in the frequency range 0.1 and 34 Hz and the peak ground acceleration (PGA) are taken as dependent variables of the regression analysis. The two horizontal components are considered as individual data. The M_L magnitude and the hypocentral distance are the independent variables of the regression analysis.

In our dataset, the PSV and the PGA levels depend on the location of the receivers in depth. The prediction attenuation relations used are assumed to have the following forms:

$$\text{Log(PSA(f))} = a(f)\, M_L - \text{Log(X)} + b(f)\, X + c_j(f) \qquad (j = 1,\ldots,5)$$
$$\text{Log(PGA)} = a\, ML - \text{Log(X)} + b\, X + cj \qquad (j = 1,\ldots,5)$$

Regression coefficients and standard errors are listed in Table II, for the horizontal seismic motion (5% damping for response spectra). Coefficients were computed from 0.1 to 34 Hz. We propose the linear relation $M_S = 1.154\, M_L - 1.34$ (based on the selected events) in order to use this attenuation relation with M_S.

Table II. Horizontal ground motion prediction equation coefficients (5% damping)

Freq. (Hz)	a	b	c1	c2	c3	c4	c5	sigma
0.100	0.8784	0.0018	-4.2088	-4.2006	-4.2010	-4.2108	-4.2423	0.2973
0.111	0.8991	0.0019	-4.2320	-4.2243	-4.2187	-4.2320	-4.2662	0.3005
0.125	0.9033	0.0019	-4.1517	-4.1439	-4.1359	-4.1466	-4.1945	0.3035
0.143	0.9225	0.0018	-4.1320	-4.1258	-4.1243	-4.1288	-4.1902	0.3089
0.167	0.9530	0.0014	-4.1466	-4.1444	-4.1531	-4.1381	-4.2058	0.3092
0.182	0.9476	0.0015	-4.0386	-4.0396	-4.0451	-4.0218	-4.0925	0.3116
0.200	0.9369	0.0011	-3.8728	-3.8724	-3.8801	-3.8502	-3.9244	0.3027
0.222	0.9280	0.0005	-3.6965	-3.6919	-3.6961	-3.6702	-3.7497	0.2957
0.250	0.9084	0.0002	-3.4674	-3.4628	-3.4759	-3.4442	-3.5202	0.2959
0.263	0.9152	0.0003	-3.4641	-3.4587	-3.4706	-3.4396	-3.5145	0.2922
0.278	0.9125	0.0006	-3.4187	-3.4110	-3.4217	-3.3893	-3.4661	0.2937
0.294	0.9046	0.0007	-3.3294	-3.3201	-3.3337	-3.3016	-3.3764	0.2918
0.300	0.9040	0.0006	-3.3037	-3.2951	-3.3108	-3.2793	-3.3513	0.2897
0.312	0.9032	0.0004	-3.2561	-3.2479	-3.2643	-3.2303	-3.3040	0.2838
0.333	0.8987	0.0002	-3.1727	-3.1645	-3.1781	-3.1463	-3.2201	0.2786
0.357	0.8928	-0.0002	-3.0776	-3.0702	-3.0853	-3.0494	-3.1283	0.2873
0.385	0.8878	-0.0007	-2.9780	-2.9650	-2.9837	-2.9459	-3.0303	0.2915
0.400	0.8790	-0.0008	-2.8886	-2.8764	-2.8951	-2.8560	-2.9416	0.2933
0.417	0.8618	-0.0008	-2.7454	-2.7375	-2.7541	-2.7177	-2.8022	0.2927
0.455	0.8319	-0.0008	-2.4961	-2.4892	-2.5061	-2.4702	-2.5575	0.2894
0.500	0.8201	-0.0004	-2.3716	-2.3671	-2.3852	-2.3485	-2.4401	0.2983
0.556	0.7921	0.0001	-2.1678	-2.1644	-2.1874	-2.1449	-2.2452	0.3043
0.600	0.7873	0.0000	-2.0613	-2.0599	-2.0839	-2.0390	-2.1485	0.3177
0.625	0.7808	-0.0003	-1.9687	-1.9675	-1.9880	-1.9474	-2.0590	0.3187
0.667	0.7735	-0.0006	-1.8472	-1.8438	-1.8655	-1.8257	-1.9383	0.3296
0.700	0.7674	-0.0009	-1.7545	-1.7524	-1.7770	-1.7365	-1.8522	0.3395
0.714	0.7630	-0.0010	-1.7055	-1.7034	-1.7282	-1.6892	-1.8063	0.3400
0.769	0.7316	-0.0004	-1.5065	-1.5011	-1.5270	-1.4944	-1.6107	0.3242
0.800	0.7164	0.0000	-1.4149	-1.4130	-1.4377	-1.4109	-1.5275	0.3133
0.833	0.7010	0.0003	-1.3111	-1.3091	-1.3350	-1.3132	-1.4345	0.3079
0.900	0.6823	0.0010	-1.1846	-1.1865	-1.2142	-1.1961	-1.3324	0.3016
0.909	0.6816	0.0011	-1.1755	-1.1771	-1.2047	-1.1871	-1.3259	0.3012
1.000	0.6686	0.0010	-1.0416	-1.0433	-1.0732	-1.0623	-1.2116	0.2998
1.100	0.6142	0.0014	-0.7024	-0.7041	-0.7386	-0.7398	-0.8951	0.3045
1.111	0.6086	0.0015	-0.6707	-0.6717	-0.7067	-0.7090	-0.8665	0.3048
1.176	0.5865	0.0019	-0.5266	-0.5258	-0.5631	-0.5720	-0.7431	0.3003
1.200	0.5831	0.0020	-0.4993	-0.4988	-0.5360	-0.5498	-0.7241	0.2954
1.250	0.5751	0.0021	-0.4349	-0.4363	-0.4750	-0.4979	-0.6764	0.2859
1.300	0.5703	0.0021	-0.3899	-0.3963	-0.4383	-0.4700	-0.6563	0.2844
1.333	0.5669	0.0022	-0.3604	-0.3694	-0.4137	-0.4504	-0.6427	0.2889
1.400	0.5557	0.0023	-0.2793	-0.2922	-0.3389	-0.3849	-0.5897	0.2936
1.429	0.5447	0.0023	-0.2099	-0.2250	-0.2732	-0.3207	-0.5315	0.2925
1.471	0.5260	0.0024	-0.0949	-0.1104	-0.1625	-0.2131	-0.4324	0.2899
1.500	0.5159	0.0025	-0.0311	-0.0464	-0.1006	-0.1544	-0.3791	0.2875
1.515	0.5108	0.0026	0.0001	-0.0152	-0.0708	-0.1265	-0.3536	0.2865
1.562	0.4973	0.0028	0.0791	0.0637	0.0061	-0.0552	-0.2915	0.2818
1.600	0.4888	0.0031	0.1282	0.1114	0.0527	-0.0131	-0.2548	0.2767
1.613	0.4872	0.0032	0.1386	0.1213	0.0625	-0.0054	-0.2488	0.2753

Freq. (Hz)	a	b	c1	c2	c3	c4	c5	sigma
1.667	0.4838	0.0034	0.1659	0.1472	0.0850	0.0083	-0.2411	0.2739
1.700	0.4815	0.0035	0.1877	0.1677	0.1026	0.0205	-0.2323	0.2732
1.724	0.4792	0.0035	0.2085	0.1885	0.1210	0.0351	-0.2209	0.2717
1.786	0.4780	0.0034	0.2405	0.2204	0.1478	0.0543	-0.2104	0.2680
1.800	0.4790	0.0034	0.2408	0.2203	0.1465	0.0519	-0.2150	0.2672
1.852	0.4848	0.0032	0.2318	0.2086	0.1298	0.0288	-0.2380	0.2646
1.900	0.4880	0.0031	0.2318	0.2073	0.1236	0.0168	-0.2465	0.2629
1.923	0.4879	0.0031	0.2387	0.2135	0.1278	0.0187	-0.2429	0.2625
2.000	0.4869	0.0030	0.2591	0.2295	0.1389	0.0229	-0.2300	0.2592
2.083	0.4835	0.0028	0.2883	0.2560	0.1557	0.0358	-0.2012	0.2554
2.100	0.4825	0.0028	0.2971	0.2644	0.1622	0.0415	-0.1924	0.2548
2.174	0.4729	0.0026	0.3607	0.3263	0.2150	0.0894	-0.1265	0.2560
2.200	0.4684	0.0025	0.3899	0.3543	0.2414	0.1140	-0.0970	0.2564
2.273	0.4538	0.0024	0.4799	0.4420	0.3222	0.1916	-0.0058	0.2572
2.300	0.4502	0.0023	0.5052	0.4669	0.3443	0.2113	0.0198	0.2569
2.381	0.4446	0.0021	0.5577	0.5151	0.3868	0.2446	0.0716	0.2539
2.400	0.4441	0.0021	0.5658	0.5225	0.3926	0.2480	0.0796	0.2532
2.500	0.4409	0.0019	0.6033	0.5580	0.4216	0.2662	0.1195	0.2511
2.600	0.4356	0.0016	0.6519	0.6056	0.4606	0.2977	0.1688	0.2551
2.632	0.4338	0.0016	0.6666	0.6196	0.4726	0.3081	0.1852	0.2565
2.700	0.4331	0.0014	0.6797	0.6309	0.4788	0.3108	0.2063	0.2576
2.778	0.4314	0.0013	0.7008	0.6487	0.4883	0.3155	0.2344	0.2582
2.800	0.4307	0.0013	0.7072	0.6541	0.4919	0.3189	0.2432	0.2582
2.900	0.4302	0.0011	0.7214	0.6649	0.4930	0.3229	0.2718	0.2577
2.941	0.4306	0.0011	0.7236	0.6644	0.4892	0.3206	0.2796	0.2571
3.000	0.4288	0.0010	0.7391	0.6759	0.4947	0.3299	0.3024	0.2555
3.125	0.4197	0.0010	0.7921	0.7243	0.5310	0.3732	0.3763	0.2539
3.155	0.4175	0.0010	0.8055	0.7370	0.5409	0.3840	0.3947	0.2542
3.300	0.4090	0.0009	0.8687	0.7949	0.5842	0.4387	0.4733	0.2517
3.333	0.4074	0.0008	0.8831	0.8081	0.5943	0.4517	0.4895	0.2503
3.448	0.3996	0.0007	0.9365	0.8580	0.6371	0.5013	0.5502	0.2452
3.571	0.3901	0.0008	0.9946	0.9112	0.6799	0.5544	0.6124	0.2402
3.600	0.3883	0.0008	1.0060	0.9211	0.6877	0.5655	0.6242	0.2392
3.800	0.3807	0.0007	1.0636	0.9748	0.7236	0.6187	0.6780	0.2338
3.850	0.3793	0.0007	1.0761	0.9859	0.7315	0.6299	0.6885	0.2323
4.000	0.3793	0.0005	1.0951	0.9971	0.7316	0.6469	0.7007	0.2277
4.167	0.3820	0.0002	1.1011	0.9954	0.7189	0.6537	0.6964	0.2246
4.200	0.3821	0.0001	1.1048	0.9980	0.7201	0.6574	0.6977	0.2241
4.400	0.3795	-0.0003	1.1442	1.0276	0.7482	0.7049	0.7230	0.2231
4.550	0.3758	-0.0005	1.1770	1.0531	0.7748	0.7462	0.7441	0.2250
4.600	0.3750	-0.0005	1.1843	1.0581	0.7803	0.7556	0.7485	0.2252
4.800	0.3733	-0.0007	1.2003	1.0669	0.7943	0.7819	0.7577	0.2252
5.000	0.3728	-0.0008	1.2074	1.0665	0.8002	0.8001	0.7585	0.2250
5.250	0.3719	-0.0011	1.2131	1.0607	0.8075	0.8205	0.7645	0.2224
5.263	0.3717	-0.0011	1.2140	1.0610	0.8085	0.8223	0.7656	0.2223
5.500	0.3628	-0.0011	1.2572	1.0925	0.8547	0.8779	0.8108	0.2196
5.556	0.3600	-0.0011	1.2703	1.1036	0.8705	0.8946	0.8251	0.2191
5.750	0.3535	-0.0012	1.3057	1.1297	0.9147	0.9410	0.8611	0.2185
5.882	0.3513	-0.0014	1.3225	1.1379	0.9357	0.9617	0.8760	0.2196

Freq. (Hz)	a	b	c1	c2	c3	c4	c5	sigma
6.000	0.3498	-0.0015	1.3374	1.1460	0.9537	0.9750	0.8882	0.2208
6.250	0.3482	-0.0017	1.3571	1.1542	0.9797	0.9875	0.8997	0.2215
6.500	0.3494	-0.0018	1.3564	1.1405	0.9860	0.9762	0.8905	0.2209
6.667	0.3494	-0.0019	1.3595	1.1345	0.9927	0.9736	0.8866	0.2219
6.750	0.3491	-0.0019	1.3624	1.1329	0.9971	0.9727	0.8860	0.2228
7.000	0.3484	-0.0019	1.3644	1.1267	1.0050	0.9680	0.8826	0.2248
7.143	0.3484	-0.0019	1.3620	1.1203	1.0046	0.9638	0.8798	0.2262
7.250	0.3482	-0.0019	1.3609	1.1164	1.0061	0.9617	0.8804	0.2276
7.500	0.3459	-0.0019	1.3685	1.1150	1.0210	0.9678	0.8908	0.2304
7.692	0.3431	-0.0019	1.3822	1.1228	1.0382	0.9809	0.9068	0.2305
7.750	0.3424	-0.0019	1.3858	1.1252	1.0428	0.9844	0.9116	0.2302
8.000	0.3395	-0.0019	1.3984	1.1326	1.0605	0.9997	0.9314	0.2284
8.333	0.3383	-0.0020	1.4010	1.1274	1.0659	1.0027	0.9422	0.2276
8.500	0.3389	-0.0021	1.3963	1.1179	1.0609	0.9967	0.9404	0.2268
9.000	0.3379	-0.0021	1.3886	1.1059	1.0601	0.9879	0.9353	0.2246
9.091	0.3380	-0.0021	1.3854	1.1029	1.0574	0.9851	0.9317	0.2249
9.500	0.3416	-0.0021	1.3558	1.0767	1.0274	0.9532	0.8958	0.2267
10.000	0.3440	-0.0021	1.3255	1.0589	0.9975	0.9274	0.8609	0.2318
10.500	0.3429	-0.0020	1.3131	1.0615	0.9829	0.9225	0.8518	0.2372
11.000	0.3431	-0.0019	1.2952	1.0590	0.9579	0.9103	0.8411	0.2398
11.111	0.3434	-0.0018	1.2896	1.0585	0.9526	0.9072	0.8385	0.2399
11.500	0.3429	-0.0018	1.2791	1.0653	0.9438	0.9046	0.8366	0.2407
11.765	0.3424	-0.0018	1.2738	1.0696	0.9391	0.9059	0.8364	0.2401
12.000	0.3411	-0.0017	1.2733	1.0765	0.9397	0.9104	0.8399	0.2394
12.500	0.3396	-0.0016	1.2651	1.0809	0.9352	0.9080	0.8352	0.2369
13.000	0.3403	-0.0016	1.2458	1.0770	0.9221	0.8941	0.8175	0.2350
13.333	0.3414	-0.0015	1.2272	1.0671	0.9095	0.8796	0.8023	0.2346
13.500	0.3424	-0.0015	1.2158	1.0583	0.9007	0.8700	0.7918	0.2343
14.000	0.3471	-0.0014	1.1728	1.0209	0.8644	0.8302	0.7486	0.2337
14.286	0.3506	-0.0014	1.1448	0.9970	0.8400	0.8034	0.7209	0.2334
14.500	0.3526	-0.0014	1.1277	0.9825	0.8259	0.7872	0.7053	0.2334
15.000	0.3543	-0.0013	1.1044	0.9665	0.8122	0.7652	0.6889	0.2330
15.385	0.3544	-0.0012	1.0931	0.9599	0.8077	0.7552	0.6824	0.2329
16.000	0.3565	-0.0012	1.0665	0.9353	0.7885	0.7327	0.6595	0.2359
16.667	0.3603	-0.0010	1.0281	0.8980	0.7539	0.6989	0.6197	0.2389
17.000	0.3620	-0.0010	1.0117	0.8812	0.7391	0.6854	0.6017	0.2396
18.000	0.3681	-0.0009	0.9638	0.8329	0.6929	0.6408	0.5501	0.2386
18.868	0.3720	-0.0008	0.9305	0.7993	0.6613	0.6083	0.5199	0.2376
20.000	0.3758	-0.0007	0.8949	0.7637	0.6245	0.5692	0.4857	0.2365
22.000	0.3851	-0.0006	0.8202	0.6908	0.5521	0.4908	0.4102	0.2361
25.000	0.3929	-0.0004	0.7610	0.6298	0.4940	0.4307	0.3465	0.2363
28.000	0.3959	-0.0002	0.7195	0.5984	0.4635	0.3928	0.3130	0.2329
29.412	0.3970	-0.0001	0.7041	0.5856	0.4508	0.3796	0.3006	0.2318
31.000	0.3979	-0.0001	0.6904	0.5730	0.4421	0.3677	0.2919	0.2312
33.333	0.3980	0.0000	0.6803	0.5633	0.4398	0.3605	0.2859	0.2320
34.000	0.3982	0.0000	0.6768	0.5600	0.4382	0.3575	0.2833	0.2319
PGA	0.41296	0.0003	0.5120	0.3983	0.2576	0.1962	0.1129	0.2331

For the 4 groups of (magnitude-distance) plotted on Figure 3, we have compared on Figure 4 the response spectra predicted by the attenuation relation and the actual data of each group at the five depth.

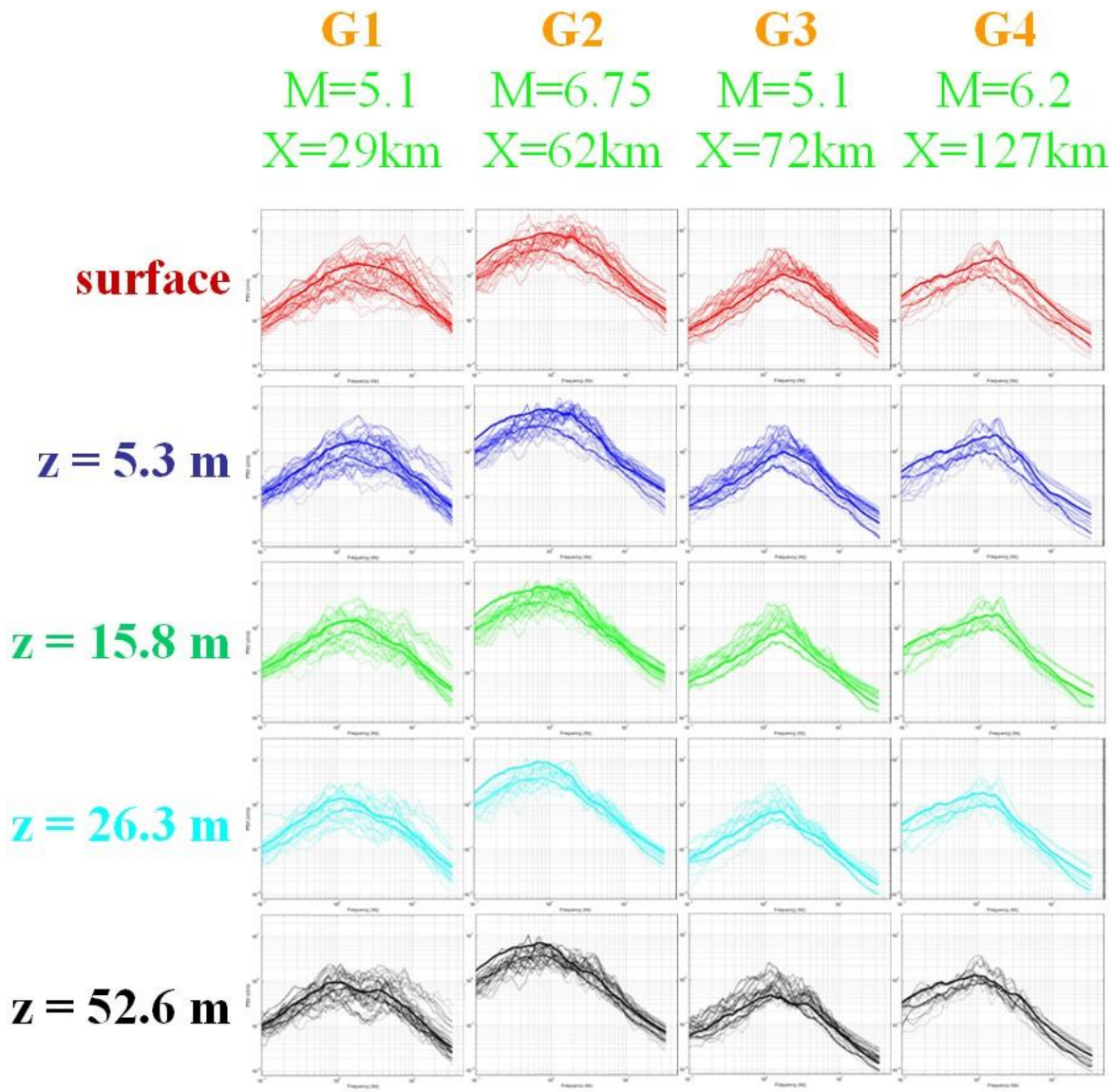

Figure 4. (Thin curves) actual data response spectra (see Figure 3 for group associations). (Thick solid curves) Horizontal spectra from the ground motion prediction equation. (Thick dotted lines) vertical spectra.

For these four groups the fit is good. We observe that for large earthquakes (group 2) the simulations slightly overestimate the true values at low frequency probably due to a non-linearity of the a(f) parameter with magnitude not taken into account in the model (Fukushima et al., 2003).
We can also notice on Figure 4 that the difference between horizontal and vertical response spectra decreases as depth increases.

4. Seismic attenuation with depth at Hualien LSST

The ratio of frequency-dependent receiver coefficients between underground and surface receivers provided an estimate of the amplitude variation between two considered depths. In Figure 5 these amplitudes variations are represented for the horizontal component in comparison with the surface motion for the 4 considered depths as a function of frequency.

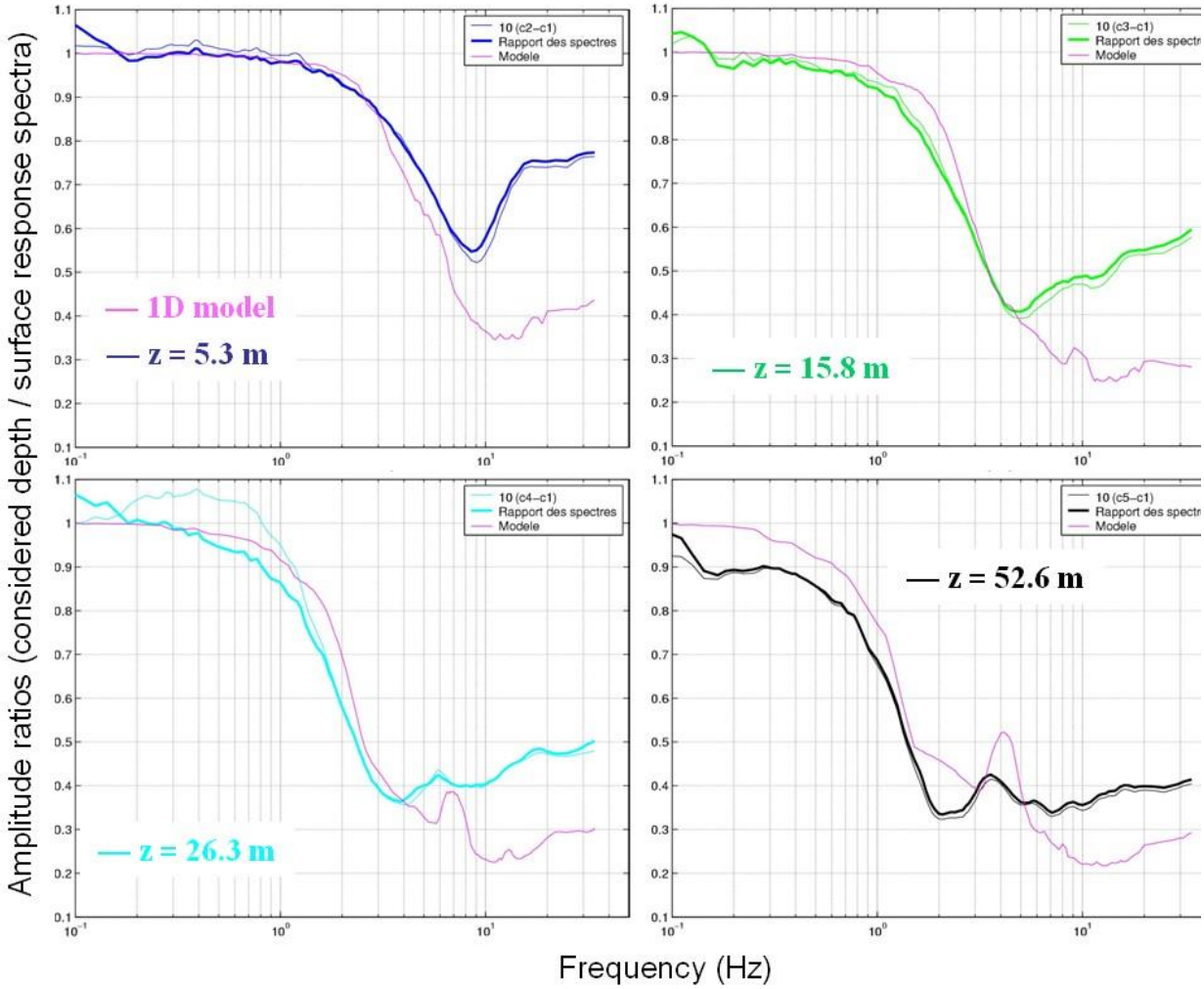

Figure 5. (Thin colored lines) Ratios of receiver coefficients of the attenuation relation. (Thick colored lines) averaged data ratios. (Pink lines) Theoretical 1D vertical SH waves ratios.

The attenuation with depth is also estimated using spectral ratios. The amplitude attenuation observed on the horizontal data can be reproduced up to 5 Hz considering a simple 1-D elastic model of SH plane waves as it is shown on Figure 5. The misfit at high frequency may be due to small scale heterogeneities not taken into account in the model.

5. Conclusions

Using about 1000 accelerometric records from two vertical arrays of the Hualien LSST, Taiwan, we derived attenuation relationships at subsurface sites (with depth ranging from 5.3 to 52.6 m) for both peak acceleration and response spectra.
The seismic motion amplitude decreases with depth. The attenuation value strongly depends on frequency and considered depth.
A 1-D elastic model of SH plane waves with vertical incidence reproduces the attenuation factor observed on horizontal components up to 5 Hz.

6. References

Angelier J., (1986) Geodynamics of the Eurasia-Philippine Sea Plate boundary : *preface Tectonophysics 125*, no 1-3, ix-x.

Bouchon M., (1981) A simple method to calculate Green's function for layered media *Bulletin of the Seismological Society of America 71*, 959-971.

Fukushima Y., C. Berge-Thierry, P. Volant, D. Griot-Pommera and F. Cotton (2003) Attenuation relation for west Eurasia determined with recent near fault records from California, Japan and Turkey. *Journal of Earthquake Engineering 7* (4), 573-598.

Fukushima Y., J.-C. Gariel and R. Tanaka (1995) Site-dependent attenuation relations of seismic motion parameters at depth using borehole data. *Bulletin of the Seismological Society of America 85 (6)*, 1790-1804.